Journal of Engineering and Sustainable Development
http://jeasd.uomustansiriyah.edu.iq
https://doi.org/10.31272/jeasd.24.6.6

JEASD

Vol. 24 No. 06, November 2020
ISSN 2520-0917

EXPERIMENTAL AND THEORETICAL OPTIMAL REGULATOR CONTROL OF BALANCE ZERO MOMENT POINT FOR BIPEDAL ROBOT

***Ali Fawzi Abdul Kareem[1]** **Ahmed Abdul Hussein Ali[2]**

1) PhD student, Mechanical Engineering Department, College of Engineering, University of Baghdad, Baghdad, Iraq.
2) Prof. Dr., Mechanical Engineering Department, College of Engineering, University of Baghdad, Baghdad, Iraq.

Received 5/2/2020 ***Accepted in revised form 21/6/2020*** ***Published 1/11/2020***

Abstract: In this paper, the optimal control is analyzed to compare the results of the zero moment point of a bipedal walking robot. Seventeen degrees of freedom bipedal walking robot is manufactured of hard Aluminum sheets. The zero moment point is calculated experimentally and theoretically in the single support phase. MATLAB Simulink is used to simulate the results. The experimental results showed that the lower link takes the settling time is (1) sec, the middle link takes settling time (0.9) sec and the upper link takes (1.1) sec to arrive the desired zero moment point for the bipedal walking robot. The minimum performance index in the experimental parts occurs when the optimal feedback control gain is [35.5 30.4 5 -4]. Hence, the minimum performance index in the theoretical part is [35 31 5.2 -4]. The dimensions of the foot area are (12.3cm×6.3cm), 2.3cm thickness, and 32g weight. Also, the approximate balance area in the double support phase equals the area between the feet of the robot.

Keywords: *Experimental optimal balance, theoretical optimal control, optimal zero moment point, experimental zero moment point, theoretical zero moment point.*

1. Introduction

The pioneering works in the field of bipedal robots were proposed around the 1970s by two famous researchers, Vukobratovic and Kato [1]. Legged robots are divided into several types included: one leg, two-legged (bipedal or humanoid), quadruped robot, and multi-legged robot. In this work, the bipedal robot or two-legged robot is used.

The bipedal robot is a serious alternative for using robots for the reason of the world's land area is unpaved. Also, a bipedal robot is better and specialized suitable to the flat surface and they can drive navigate and faster with better precision in the walking. The bipedal robot follows nature by existence capable to navigate even ascend stairs and rough terrain or above the obstacles in standard household regions.
The legged robots with three legs or more legs have the advantage of stability. The walking pattern of a six-legged robot, three legs are moving at all times, while the other legs are on the ground. This provides the robot's center of mass CoM is within a triangle-shaped by three legs on the ground that gives a static balance during the walking [1]. The bipedal robot is the hot and fascinating objects of experimentations by engineers and scientists. Several kinds of humanoids are obtainable to depend on the function, morphologies, movement, and application.

**Corresponding Author*:a.abdulkareem0903@coeng.uobaghdad.edu.iq

All kinds have a dynamic model and a static model. Most of the researchers studied the problem of the stability of a bipedal robot (Humanoid). The Humanoid is normally unstable [2], a considerable deal of overwork requires to spend on including that the control system backward the brain of the locomotion is robust and efficient. There are several sources for control problems in the bipedal robots. The selection and structure of algorithms are to fulfill different criteria like balance, energy distribution, energy efficiency and velocity [2].

One of the main control problems is biped walking because of furthermore the discrete changes in the kinetic and kinematic phenomena, the highly-coupled non-linear dynamics and high order during the gait cycle [3]. The bipedal robot walks if the CoM isn't in a vertical line above the contact area of the bipedal robot on the ground. Therefore, the CoM must be naturally moved above the leg before the second leg is moving.

Then, the possibility is the quasi-dynamic stability in this case, where the CoM is moving through the swing phase in that way that the moment for tumbling is compensated by putting the second leg on the ground again [3]. The important and basic parameter that used to meet in design a humanoid is the stability of mass concerning its CoM. Our approximation is, to begin with a pre-programmed-semi-balance for a bipedal robot.

2. Methodology

2.1. Zero Moment Point Principles

In this section, the principles of zero moment point ZMP displacements for a single support phase and double support phase are discussed. The movement of legs is utilized as an important part of the dynamics. The required data are concerned on the basis of biometric estimations of a normal human gait.

Time trajectories of the variation of angles of the knee, ankle, and hip joint in external coordinates are estimated in the course of a single support phase SSP and a full-step gait. "Fig. 1" shows that the phases of foot contact on the ground where the supporting point may be either below the heel (phase I), below the foot (phase II) and below the toes (phase III).

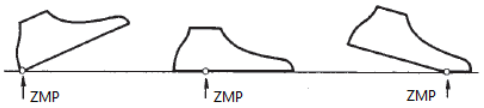

Figure 1. The phases of the bipedal robot foot in the support phase [4].

Also, the law of the ZMP displacement may be performed as follows: in the beginning of phase I the ZMP below the heel; at the end of phase I, it jumps to the foot center; at the end of phase II it's changed below the toes; at the end of the half-phase the ZMP jumps below the other foot which is now being in contact with the ground [4]. To estimate ZMP for a bipedal robot, forward kinematics hypotheses that have to be made [5].

a) The bipedal walking robot consists of n links.
b) All kinematic assumptions, such as link orientation, the position of CoM and velocities are identified and estimated by forward kinematics.
c) The ground is motionless and rigid.
d) The foot can't slide over the ground.
e) The joint is actively actuated.

Under these restrictions, the first thing to estimate is total mass m_{tot} of the bipedal robot and p is the distance from center of link to the base-frame-origin [5]:

$m_{tot} = \sum_{i=1}^{n} m_i$ (1)

p_{CoM} is the distance from the base-frame-origin to its CoM and a graphical interpretation is illustrated in "Fig. 2". "Fig. 2" describes the bipedal robot as links of rigid body [5].

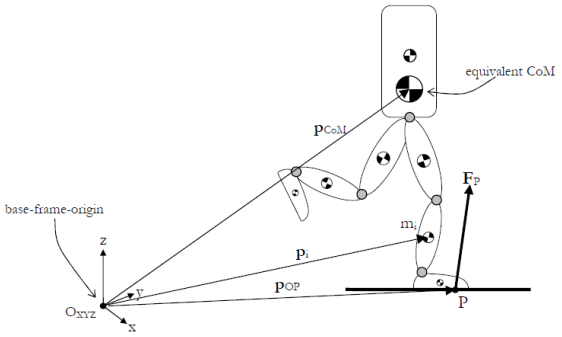

Figure 2. Schematic 3-D biped model and point *p* [5].

P and H are the total linear momentum and total angular momentum with respect of the base-frame-origin respectively can be stated as [5]:

$P = \sum_{i=1}^{n} m_i \dot{p}_i$ (2)

$H = \sum_{i=1}^{n} \{p_i \times m_i \dot{p} + I_i \omega_i\}$ (3)

Where ω_i and I_i are the angular velocity and the inertia tensor of the i-th link respectively w.r.t. the base-frame-origin [5].

For I_i the following equation holds:

$I_i = R_i I_i R_i^T$ (4)

Where I_i is the inertia matrix of the i-th link w.r.t. the base-frame-origin and R_i is the rotation matrix of i-th link with respect to the base-frame-origin attached to their links [5].

The time derivative of H and P are the rate of change of angular momentum and linear momentum (being a moment and a force), respectively. They can be stated as [5]:

$\dot{P} = \sum_{i=1}^{n} m_i \ddot{p}_i$ (5)

$\dot{H} = \sum_{i=1}^{n} (\dot{p}_i \times (m_i \dot{p}_i) + p_i \times (m_i \ddot{p}_i) + I_i \dot{\omega}_i + \omega_i \times (I_i \omega_i))$ (6)

Where $\dot{p}_i \times (m_i \dot{p}_i)$=0 because $\dot{p}_i$and $(m_i \dot{p}_i)$ are parallel (note that $(m_i \dot{p}_i)$ a scalar multiplication of $(\dot{p}_i)$ [5]. With this assumptions the following holds:

$F_p = -F_A = \dot{P} - m_{tot} g$ (7)

$M_o = \dot{H} - p \times m_{tot} g$ (8)

Where, as said earlier M_o and F_p are the moment and external force that characterize how the ground is reacting to the biped w.r.t. base-frame-origin. F_A is the force that the bipedal robot is acting upon the floor [5]. Also, the M_o is:

$M_o = p_{op} \times F_p + M_p$ (9)

Where p_{op} is the vector from the base-frame-origin to point p and M_p is the moment at p. Because M_p is on the point p, being either ZMP, its M_p= [0 0 M_z] [5]. Now, we can substitute "(8)" into "(9)" resulting in:

$M_p = \dot{H} - p_{CoM} \times m_{tot} g + (\dot{P} - m_{tot} g) \times p_{op}$ (10)

From this, the distance from location of the ZMP to the base-frame-origin $p_{zmp} = p_{op} = [x_{ZMP}, y_{ZMP}, z_{ZMP}]$ can be calculated [5]:

$x_{ZMP} = \frac{m_{tot} g_z p_{CoMx} + z_{ZMP} \dot{P}_x - \dot{H}_y}{m_{tot} g_z + \dot{P}_z}$ (11)

$y_{ZMP} = \frac{m_{tot} g_z p_{CoMy} + z_{ZMP} \dot{P}_y - \dot{H}_x}{m_{tot} g_z + \dot{P}_z}$ (12)

Where x_{ZMP} and y_{ZMP} are the distances from ZMP to the base-frame-origin about x-axis and y-axis respectively. Remind that z_{ZMP} is the height of the floor. When the XY-plane is placed on the floor z_{ZMP}becomes zero [5].

For measuring ZMP experimentally, the load cell is used and connect with the HX711 sensor

as shown in "Fig. 3". In this work, 50 kg body load cell weighing sensor resistance strain half-bridge is used to measure the load that applied from the feet on the ground.

This load cell operates at minute voltage changes and needs HX 711 amplifier load cell. The internal 1000 ohm half-bridge strain gauge, half-bridge structure, the measuring range is 50 kg weighing sensor. When measuring, the force should be applied to the outer side of the strain E-shaped portion of the sensor and the outsides edges to form a shearing force in the opposite direction.

Mount the load cells to the bottom of the scale in the four corners. Epoxy works well to hold them in place. The load cell has three wires (white, red and black) and the dimensions are (34*34*7.8 mm). For connecting the HX711 amplifier with the Arduino microcontroller, the procedures can be followed as shown in "Fig. 3":

1- GND GND

2- VCC VCC

3- DT digital PWM

4- SCK digital PWM

"(13)" is used to estimate the zero moment point experimentally [6]:

$$ZMP = \frac{\sum_{i=1}^{4} F_i r_i}{\sum_{i=1}^{4} F_i} \quad (13)$$

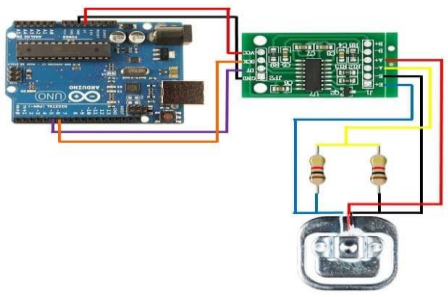

Figure 3. Connection load cell sensor with hx711 amplifier to Arduino microcontroller.

Where F_i forces implemented on the sensors and r_i sensor positions are as illustrated in "Fig. 4" and O is the origin of the foot coordinate frame. In the double support phase, to obtain the zero moment point coordinates, the zero moment point readings of the two feet are interpolated by weighting them by the total forces applied to the right and left sensor sets [6]. For estimating the load, load cell, and HX711 load cell amplifiers are utilized and connected with Arduino microcontroller UNO and discussed in detail below.

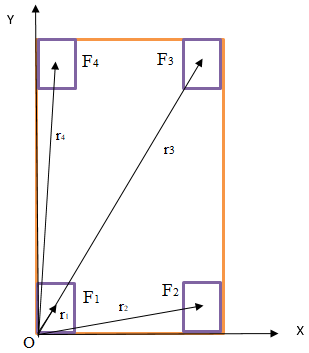

Figure 4. The placement of the load cell under the foot.

2.2. Optimal Control Method

In ZMP-based controlled humanoid, if the ZMP is approaching the support area between the feet on the ground, it is concluded that robot is going to fall and controlling the balance stability is achieved by keeping zero moment point as far as possible from boundaries of support area [7].

"Fig. 5" shows the optimal control system where is an important assignment of control engineering. The optimal control aims to understand a system that will prepare the desired J. So, transient response parameters such as the rise time and max overshoot are considerable of J. The J is expressed as the state variables of a system in a general form as:

$$J = \int_0^{t_f} g(x,u,t)dt$$

Where the state vector is x, and the control vector is u,and t_f is the final time.

To get the appropriate design of optimal control, J must be minimized [8, 9]. To be useful, the J must be a number that's always zero or positive. Also, the purpose of the linear quadratic regulator LQR method is to implement a regular way of estimating the $u(t)$ [10, 11]. The Hamilton-Jacobi matrix is ordinarily determined for the special and important case of the linear time-invariant transfer function with J; which takes the form of the Riccati equation.

There are several kinds of an optimal control problem, the terminal control, the minimum time control, the minimum energy, the regulator control, and the tracking control problems. The determination on the kind of J to be chosen based on the variety of the control problem.

Conventionally, the bipedal walking robot is prepared for walking which is to reduce the error $\varphi_e(t)$ between the required value of ZMP and the actual value of the angle θ in the presence of disturbances. To transfer the state vector to the required a limited region of the state space and design an allowable control vector $u(t)$, the optimal control is investigated.

For the existence of an allowable $u(t)$, the system must be completely controllable. For compensation the noise effects, the optimal control is designed in the time domain. The frequency response must be reduced highly in the frequency range where resonance and noise of components are predictable. To get a fast response; q_{11}, must be larger than q_{22}, q_{33},…etc and R [11].

The system equation is

$$\dot{x} = Ax + Bu \tag{14}$$

Now, to find the matrix K of the optimal control vector

$$u(t) = -Kx(t) \tag{15}$$

So as to minimize the J is given in terms of the input vector instead of state vector, that is

$$J = \int_0^\infty (x^T Qx + u^T Ru)dt \tag{16}$$

Also, J that given in terms of the output vector, that is,

$$J = \int_0^\infty (y^T Qy + u^T Ru)dt \tag{17}$$

Napoleon proposed new theorem

$$J = \int_0^\infty (x^T Qx + y^T Qy + u^T Ru) \tag{18}$$

$$y = Cx + Du \tag{19}$$

Where Q and R are a positive-definite symmetric matrix. Note that the right-hand side from above "(17)" estimates the consumption of the energy of $u(t)$ and the error.

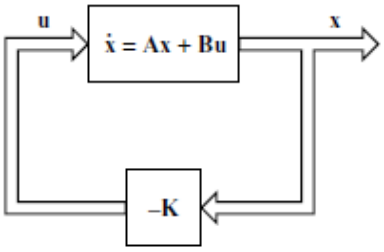

Figure 5. Optimal regulator system [11].

Therefore, if the unknown elements of the matrix $\boldsymbol{K}$ are calculated to minimize the J, then $\boldsymbol{u}(t) = -\boldsymbol{K}\boldsymbol{x}(t)$ is optimal for any initial condition $\boldsymbol{x}(0)$ and $y = Cx$. Hence, the optimal control is designed to find $u(t)$ which causes the system

$$\dot{x} = g(x(t), u(t), t) \tag{20}$$

To choose an optimal state variable $x(t)$ that minimizes J,

$$J = \int_{t_0}^{t_1} h(x(t), u(t), t)dt \tag{21}$$

To derive the performance index for a continuous system, the procedures must be followed:

$$f(x,t) = min_u \int_{t_0}^{t_1} h(x,u)dt \quad (22)$$

Where the time interval t_0 to t_1,

$$f(x,t_0) = f\big(x(0)\big)$$

$$f(x,t_1) = 0$$

From "(20)" and "(21)", Hamilton-Jacobi assumption may be distinct as

$$\frac{\partial f}{\partial t} = -min_u \left[h(x,u) + \left(\frac{\partial f}{\partial x}\right)^T g(x,u)\right] \quad (23)$$

For a linear transfer function, "(22)",

$$\dot{x} = Ax + Bu \quad (24)$$

And if "(20)" is a quadratic J

$$J = \int_{t_0}^{t_1} (x^T Qx + u^T Ru)dt \quad (25)$$

Substituting "(24)" and "(25)" into equation "(23)"

$$\frac{\partial f}{\partial t} = -min_u \left[x^T Qx + u^T Ru + \left(\frac{\partial f}{\partial x}\right)^T (Ax + Bu)\right] \quad (26)$$

Introducing an equation of the form

$$f(x,t) = x^T Px \quad (27)$$

Where P is a matrix, then

$$\frac{\partial f}{\partial t} = x^T \frac{\partial}{\partial t} Px \quad (28)$$

And

$$\frac{\partial f}{\partial x} = 2Px$$

$$\left[\frac{\partial f}{\partial x}\right]^T = 2x^T P \quad (29)$$

Inserting "(28)" and "(29)" into "(26)" gives

$$x^T \frac{\partial}{\partial t} Px = -min_u [x^T Qx + u^T Ru + 2x^T P(Ax + Bu)] \quad (30)$$

To minimize u, from "(30)"

$$\frac{\partial \left[{}^{\partial f}/_{\partial t}\right]}{\partial u} = 2u^T R + 2x^T PB = 0 \quad (31)$$

"(35)" can be re-arranged to give u_{opt},

$$u_{opt} = -R^{-1}B^T Px \quad (32)$$

Or

$$u_{opt} = -Kx \quad (33)$$

Where

$$K = R^{-1}B^T P \quad (34)$$

Substituting "(32)" back into "(30)" gives

$$x^T \dot{P}x = -x^T (Q + 2PA - PBR^{-1}B^T P)x \quad (35)$$

Since

$$2x^T PAx = x^T (A^T P + PA)x$$

Then

$$\dot{P} = -PA - A^T P - Q + PBR^{-1}B^T P \quad (36)$$

The coefficients of $P(t)$ are determined by MATLAB SIMULINK with the B.C,

$$x^T(t_1)P(t_1)x(t_1) = 0 \quad (37)$$

Kalman explained the value of J, the solution of $P(t)$ reduce to the permanent amount should t_1 must be infinity, or extracted from t_0 is zero, hence, the Ricatti equation converge to a an instantaneous equations.

$$PA + A^T P + Q - PBR^{-1}B^T P = 0 \quad (38)$$

Hence,

$$p = Cx + Du$$

$$Q = \begin{bmatrix} C^T WC & 0 \\ 0 & 0 \end{bmatrix} + \tilde{Q} \text{ and } R = D^T \widetilde{W} D + \tilde{R}$$

$$Q = \begin{bmatrix} q_{11} & 0 & 0 \\ 0 & q_{22} & 0 \\ 0 & 0 & 0 \end{bmatrix}$$

"(38)" is called the reduced-matrix Riccati equation. Riccati equation can be solved by MATLAB SIMULUNK. To get fast response, q_{11} must be larger than q_{22} and R. Hence, we proposed that $W = diag\left[\frac{1}{\theta_i^2}\right]$, $\tilde{R} = diag[\frac{1}{\ddot{\theta}_i}]$ and $\widetilde{W} = diag[\frac{1}{p^2}]$, where θ_i is the angle of LIPM (must be very small and measured by rad), $\ddot{\theta}$ is the angular acceleration (rad/s^2) and p is the ZMP (m) [12].

2.3. Calibrating of Servos by Adafruit PCA9685 16-Channel Servo Driver

Servo pulse timing changes between different models and brands. Since it is an analog control circuit, there are often some differences between specimens of the same model and brand. For accurate position control, the maximum and minimum pulse-width is calibrated in the code to match the known positions of the servo. Three factors are important for calibrating the servos by 16-channel servo driver, servo max, servo min, and frequency:

1. Servo maximum: is the maximum pulse length for a 16-channel servo driver about (600).

2. Servo minimum: is the minimum pulse length for a 16-channel servo driver about (150).

3. Frequency: is defined as how many full 'pulses' per second are generated by the IC about (40-1000 Hz).

Use attention when settling servo max and servo min. hitting the physical limits of travel permanently damage the servo because strip the gears. To convert the pulse length to the degrees, the Arduino "map ()" function is used. Assuming a typical servo with 180° position of rotating once servo max is calibrated to the 180° and servo min to 0° position. For converting any angle between 180° and 0° to the corresponding pulse length with the following line of code:

Pulse length = map (degrees, 0, 180, SERVOMIN, SERVOMAX);

The driver is programmed by setting the duty cycle and PWM frequency of each channel to accurately control servos. If we set the time of the servo_ON as 409, the period for servo_OFF would be 1228, and the duty cycle of PWM be (1228-409/4096)*100%=20% as shown in "Fig. 6".

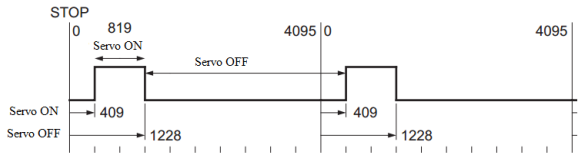

Figure 6. PWM for PCA9685 servo driver channel.

In this work, the PCA 9685 servo driver chip is used as control and can output sixteen channels of PWM signal. Pulse width modulation signals go to the signal demodulation circuit through the receiving channel and to generate a direct current DC bias voltage. It will then be compared with the voltage of the potentiometer and thus a voltage gap is concerned and input to the motor driver IC into the motors to rotate anticlockwise or clockwise direction.

When the speed reaches a certain number, it will drive the potentiometer R to rotate by the cascaded reduction gear, until the gap is reduced to zero and the servo stop spinning. A servo is controlled by PWM signals and the change of

duty cycle control that of the position the servo. PCA 9685 16-channels driver is used widely popular in robotics applications and industries.
It is controlled via PWM signal. Servo motors turn from 180°to 0° based upon the pulse width as shown in "Fig. 7". "Fig. 7" shows the angles of the pulses of servomotor with 5V. When $t =$ 0.5ms, the angle of the servomotor is 0° and the angle increases when the time increased to 2.5ms when the angle arrived to 180°.

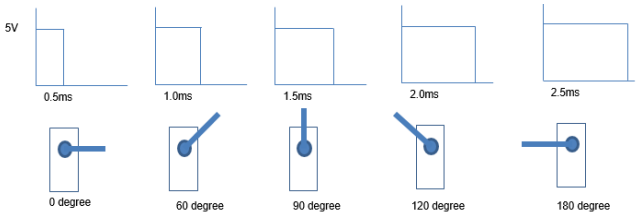

Figure 7. Angles of servomotors via PWM signals.

2.4. Kinetic of Rigid Body

Ali Fawzi and Ahmed Abdul Hussein proposed optimal control for three models of linear inverted pendulum model LIPM [12]. They found that three masses LIPM is the better regulation to the ZMP as shown in "Fig. 8" [12]. In this work, Kinetic of three linear inverted pendulum model is proposed and derived below.

For lower inverted pendulum model

$\sum M_1 = I_1 u_1 = 0$, where mass of the lower link is very small ($I_1 = 0$)

For middle inverted pendulum model

$\sum M_2 = I_2 u_2 = 0$, where mass of the middle link is very small ($I_2 = 0$)

For upper inverted pendulum model

$\sum M_3 = I_3 u_3 = 0$, where mass of the upper link is very small ($I_3 = 0$)

$$\begin{pmatrix} A & B \\ C & D \end{pmatrix} = \begin{cases} \frac{d}{dt}\begin{bmatrix}\theta \\ \dot{\theta}\end{bmatrix} = \begin{bmatrix}0 & I \\ 0 & 0\end{bmatrix}\begin{bmatrix}\theta \\ \dot{\theta}\end{bmatrix} + \begin{bmatrix}0 \\ I\end{bmatrix} u \\ p = [C_1 \quad 0]\begin{bmatrix}\theta \\ \dot{\theta}\end{bmatrix} + Du \end{cases}$$

$$G(s) = \left[\frac{d_1 s^2 + c_1}{s^2} \quad \frac{d_2 s^2 + c_2}{s^2}\right]$$

Three masses LIPM is proposed in this paper, the system involves three inputs angular accelerations (u_1, u_2, u_3) and one output ZMP (p). Three transfer functions are involved: $\frac{p}{u_1}, \frac{p}{u_2}$ and $\frac{p}{u_3}$.

Where

$$C_1 = \begin{bmatrix} \frac{m_1 l_1 + m_2 l_1 + m_2 l_2 + m_3 l_1 + m_3 l_2 + m_3 l_3}{m_1 + m_2 + m_3} & \frac{m_2 l_2 + m_3 l_2 + m_3 l_3}{m_1 + m_2 + m_3} \\ & \frac{m_3 l_3}{m_1 + m_2 + m_3} \end{bmatrix}$$

$$D = \left[-\frac{m_1 l_1^2 + m_2 (l_1 + l_2)^2 + m_3 (l_1 + l_2 + l_3)^2}{(m_1 + m_2 + m_3) g} - \frac{m_2 (l_1 + l_2) l_2 + m_3 (l_2 + l_3)(l_1 + l_2 + l_3)}{(m_1 + m_2 + m_3) g} - \frac{m_3 (l_1 + l_2 + l_3) l_3}{(m_1 + m_2 + m_3) g} \right]$$

Where $C_2 = D_2 = 0$.

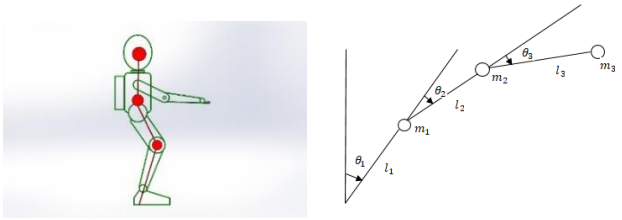

Figure 8. Three linear inverted pendulum model [12].

2.5. Controller of the Bipedal Robot

The transfer function of the DC servomotor is [14]:

$$\frac{\theta_m(s)}{E_a(s)} = \frac{K_i}{L_a J_m S^3 + (R_a J_m + B_m L_a) s^2 + (K_b K_i + R_a B_m) s} \quad (39)$$

Where

θ_m: Rotor displacement, E_a: Input voltage, K_i: Torque constant, L_a: Armature inductance, J_m: Rotor inertia, R_a: Armature resistance, B_m: Viscous-friction coefficient, K_b: Back-emf constant.

From the transfer function of the servomotor, the type of the controller of the servomotor is integral. The block diagram of the bipedal robot that used in this work as shown in "Fig. 9"

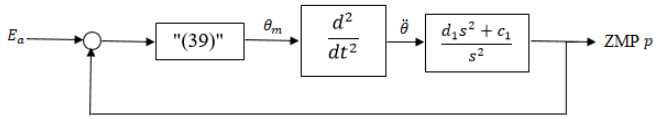

Figure 9. Block diagram of the humanoid robot.

3. Experimental Part

The design of the humanoid involves both electronics and mechanical considerations equally. So, the design and fabrication of a bipedal robot are described. Also, all the devices that used for programming the bipedal robot by Arduino are illustrated in detail. Analyzing, design, and the making of the humanoid robot will be carried out through the following steps. Conceptual designing, mathematical analysis, and components that use in the humanoid robot are explained below.

A humanoid can be mostly characterized as the kind of an independent system. The design of a bipedal robot is very important for the achievable implementation of the humanoid, especially the weight of the system imposes physical limits. The humanoid robot body is appropriate to be appointed as human substitutes and obstacle avoidance. In this work, a bipedal robot has (5 DOF) for each link, where (2 DOF) at the ankle joint, (2 DOF) at the hip joint, and (1 DOF) at the knee joint.

The design of the link for the humanoid robot is the main task because the servo motor to be included in every link. This link will be rectangular which contains several numbers of brackets connected to build a bipedal robot as shown in "Fig. 10" and "Fig.11". The servo motor will be arranged in the upper bracket and connected with the lower bracket by screws.

Two brackets are connected to create a link to the bipedal walking robot. The lower bracket is designed to move the servo motor and the servomotor will be connected to the upper bracket. The microcontroller unit transmits the program to the servo controller board bases on the movement required.

The servo controller creates a pulse width modulation signal with period PWM concerning the information received thereby rotating the servos with speed and angles as required. The following experimental setup will show the components present in a humanoid robot as shown in "Fig. 11". This work is broken into two sections hardware and software. Each section will illustrate in detail a component that used for making a bipedal robot [12].

3.1. Hardware

Bipedal robots have a combination of sensors and motors controlled by electrical circuitry called a microcontroller. The hardware consists of Arduino microcontroller UNO, high torque servomotor, and sensors. In this work, the hardware design of a new autonomous walking robot with seventeen degrees of freedom is presented. Each servo is represented a one DOF, where the head has one servomotor, two servomotors in the shoulders, each arm has two servomotors and each leg has five servomotors.

Figure 10. Black Aluminum sheets and high torque servo motor.

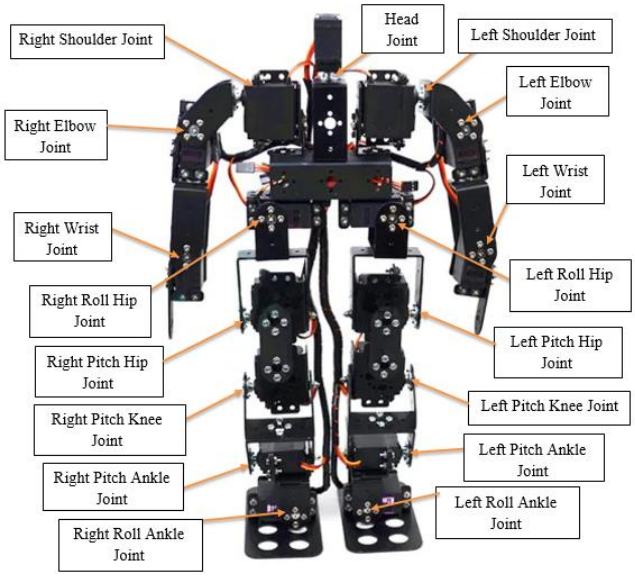

Figure 11. 17 DOF bipedal walking robot, where each joint represented a one DOF.

3.2. Software

The main concept of the software algorithm is to realize the general these states that the bipedal robots have to fulfill to maintain walk progressively and balance. The three cases are [13]:

1- Initialization

2- Balance control

3- Termination

In the initialization case, the bipedal is in a stable position. This initialization state approaches the balance to determine the mode of walking and the correct direction. The balance control case involved the changing of the robot's CoM in a toppling manner tending towards stability. In the final case, the state includes the robot to come back to the stability state as it comes out of the walking locomotion.
To discuss the autonomous of the bipedal gait algorithm a marching gait with two steps right and left, five states will assume where the bipedal robot tends to topple or tend to either balance [13]. The CoM tends to change as shown in "Fig. 12" by the cube on top of the bipedal robot. In states two and four, the bipedal robot tends to an out of stability point. If the leg bent continuously in the same direction then the robot will fall. The control algorithm should not counter the tending to fall by shifting the original leg back to the initial position.

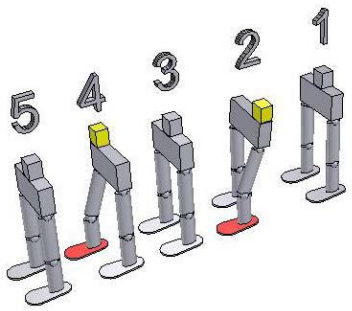

Figure 12. Hypothetical marching gait example [13].

For programming the bipedal walking robot, the Arduino microcontroller is used and connected with the PC. Firstly, battery LIPO 7.2V (2200mAh) is used to run the bipedal robot. But battery LIPO 7.2V (2200mAh) is not appropriate to run 17 DOF bipedal robots because it does not deliver the servos by the sufficient current, where the MG996R servo that used in this work is needed approximately (0.5A-0.9A). Five servos run together in any phase in the gait cycle. Battery LIPO 7.2V (2200mAh) is replaced by Battery LIPO 7.2V (6000mAh) to deliver the servos by the appropriate current. "Fig. 13" shows the main parts that need for programming the bipedal walking robot.

1- Arduino UNO'
2- Battery LIPO 7.2V (6000mAh)'
3- Voltage regulator'
4- Breadboard'
5- 16-PWM channels servo driver Adafruit 96685,
6- Gyroscope sensor.

The design concentrated firstly on the walking by using servomotors. The elementary configuration for the walking distinct the servomotors rotates about a coordinate axis of rotation, this due to instability. In this work, seventeen servomotors were also taken into consideration so that the DOF would tend to give human-like locomotion.
The humanoid has five servos for each leg and a microcontroller that is connected to the control panel. The servomotors prepare an acceptable quantity of compliance during the motion. The structure replaced with the head was used to house the controller and the payload to the robot. Microcontroller, PCA 16 servo driver channel, battery, voltage regulator and bread are connected on the fiberglass board 2mm thickness as shown in "Fig. 13".

The main structure is built from the hard aluminum bracket of 2mm thickness is used. This provides enough strength, flexibility and gives the robot lightweight. The brackets are made into different sizes of sheets to build the joint in high precision. The CoM of the humanoid is one of the significant parameters for stability. This depends on the four factors such as weight distribution, the distance between the legs and the height of the robot. Also, the rotational motion is a significant factor in the counter-balance and stability of the walking. The servo motors were located in the feet as joints to make a motion similar to the human motion.

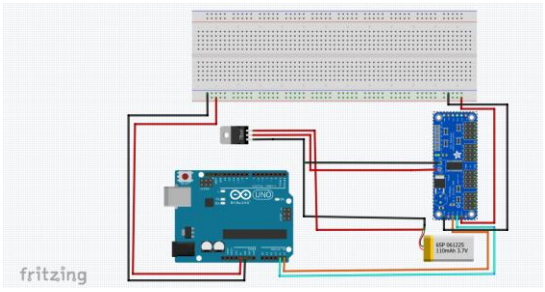

Figure 13. Control panel of the Robot.

The servomotor on the ankle joint turns the humanoid left and right while the servos on the knee and hip have the same axis of rotation. The knee and hip joints were linked to stable the humanoid about the backward and forward directions while the ankle joint was used to turn in this approach to stable the robot's CoM from side to another. The servomotors and the Arduino UNO microcontroller are connected, so a simple serial port is adequate to regulate the servomotors. The digital servomotors can act as sensors, electrical current data, and returning position when being carried the suitable command series.

The main procedures of the program include four steps:

- Starting the servomotors.

- Regulation of the servo motors to the "up" position.
- Looping between "down" and "up".
- Releasing of the servo motors.

4. Results and Discussion

Four load cells are mounted on the sole of each foot to measure ZMP while walking [14]. Besides, optimal control is used to confirm the balance of bipedal robot [15]. Also, Chengju Liu et al. (2020) developed a foot positioning compensator FPC for a bipedal robot to retrieve the stability during continuous walking [16]. Ali Fawzi and Ahmed Abdul Hussein (2019) studied the minimum performance index for three models of linear inverted pendulum model [12].

They found the three masses LIPM is the better regulation to regulate the ZMP to the desired ZMP or ZMP reference. The optimal control method for three LIPM models is selected to get a fast response to track the desired ZMP [12]. For simulation, the transient response for this control system used the linear model with differential state values to explore the applicability of the linear design.

The main parameters influencing the stability of bipedal walking robots are discovered. The results showed that the performance of three masses LIPM is satisfying because of the fast response to arrive in the desired region for a step input. A design that minimizes J represents a compromise between the conflicting desiderata of reasonably sized inputs and good regulation [12].

In this work, ZMP is determined experimentally and theoretically for a single support phase. Regulator optimal control is used to regulate the zero moment point to the desired region or reference ZMP. The error percentage between the experimental and theoretical ZMP approximately 3%.

Then, the possibility is the quasi dynamic stability in this case, where the CoM is moving through the swing phase in that way that the moment for tumbling is compensated by putting the second leg on the ground again [16]. For three LIPM as shown in "Fig. 14", the robot parameters used in the simulation are $m_1 = 0.4$ kg, $l_1 = 14\ cm$, $m_2 = 0.4kg, l_2 = 14cm, m_3 = 1kg, l_3 = 10cm$. The dimensions of the foot is ($12.3cm$ ×6.3cm), 2mm thickness, and 32g weight.

The approximate dimensions between the feet are (6cm× $12.3cm$). Hence, the approximate balance area equals the area between the feet. In the experimental results, the lower link takes the settling time is (1 sec), the middle link takes settling time is (0.9 sec) and the upper link takes (1.1 sec) to arrive the desired ZMP p of the bipedal walking robot.

The minimum performance index occurs when the optimal feedback control gain is K = [35.5 30.4 5 -4]. When J is minimized, that represents a comparison between the conflicting desiderata of the regulation and reasonably sized inputs.

In this work, the optimal stability control is designed in the time domain, it is desirable to study the frequency response identified to satisfy for noise effects. An allowable control $u(t)$ that transfers the state to the required a limited area of the state space and gives the J is minimized. Besides, the other reason for it, a three masses linear inverted pendulum and the two masses linear inverted pendulum model have a better high-frequency noise rejection, performance robust stability and better set-point tracking to the ZMP than one mass linear inverted pendulum model [17].

In the theoretical results, the lower link takes the settling time is (1.1 sec), the middle link

takes settling time is (1.1 sec) and the upper link takes (1.2 sec) to arrive the required ZMP p of the bipedal walking robot in the single support phase as shown in "Fig. 15" in phase II. The minimum performance index occurs when the optimal feedback control gain is K = [35 31 5.2 -4].

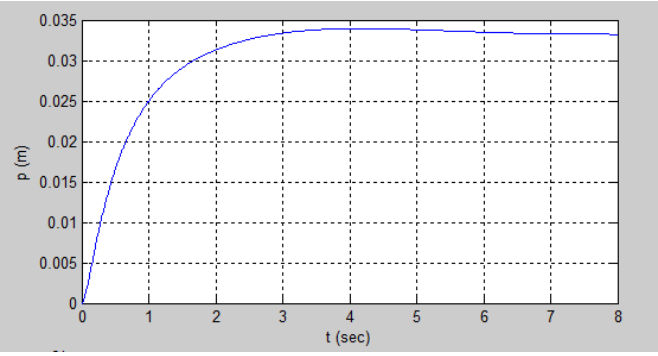

Figure 14. Experimentally optimal control of ZMP (0.034m).

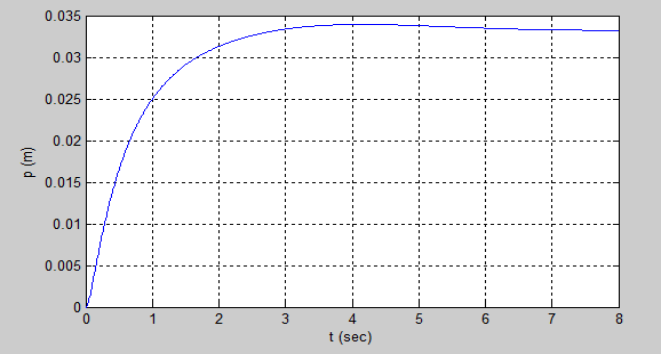

Figure 15. Theoretically optimal control of ZMP (0.033).

In this work, a method to estimate the stability area in the double support phase is proposed to use weights that minimized the performance index. This area is approximately equal to the foot area. When the performance is minimized, that means a fast response to arrive at the desired ZMP [12]. Hence, when the J is minimized, the consumption of the control signal energy is very important and must be limited to conserve energy.

So, the system is optimum only for the distinct set of I.C that was proposed. "Fig. 14" shows the experimentally transient responses for three LIPM, where the state variables $x = [x_1, x_2, x_3]$, the input is angular accelerations (u_1, u_2, u_3) and the output is ZMP p, it turns out that the initial guesses for R and Q are satisfactory [12].

5. Conclusions

The stability problem for the bipedal robot is considered. The performance index J is found to determine the desired zero moment point. For three masses LIPM, the robot parameters used in the simulation are $m_1 = 0.4$ kg, $l_1 = 14\ cm$, $m_2 = 0.4kg, l_2 = 14cm, m_3\ 1kg, l_3 = 10cm$. The dimensions of the foot are ($12.3mm$ ×6.3cm), 2mm thickness, and 32g weight. The approximate dimensions between the feet are (6cm× $12.3cm$).

Hence, the balance dimensions in the double support phase approximately equal the foot dimensions ($12.3cm$ ×6cm) or the area between the feet. In the experimental results, the lower link takes the settling time is (1 sec), the middle link takes settling time is (0.9 sec) and the upper link takes (1.1 sec) to arrive the desired ZMP p of the bipedal walking robot. The minimum performance index in the experimental part occurs when the optimal feedback control gain is K = [35.5 30.4 5 -4].

In the theoretical results, the lower link takes the settling time is (1.1sec), the middle link takes settling time is (1.1 sec) and the upper link takes (1.2 sec) to arrive the required ZMP p of the bipedal walking robot in the single support phase in phase II. Hence, the minimum performance index in the theoretical part occurs when the optimal feedback control gain is K = [35 31 5.2 -4].

Acknowledgements

A part of this research is supported by mechanical engineering/ College of Engineering/ University of Baghdad.

Conflict of interest

The authors declare that there are no conflicts of interest regarding the publication of this manuscript**.**

Nomenclature

F External force (N)

F_A The force that the bipedal robot is acting upon the ground (N)

$G(s)$ Transfer function

g Gravitational acceleration (m/s^2)

H Angular momentum (kg.m^2.rad/s)

I Moment of inertia (kg.m^2)

K Optimal gain feedback

l Length of the link (m)

m Mass of the robot (kg)

m_i Mass of the link (kg)

m_{tot} Total mass (kg)

n No. of rigid link

p Distance from the center of a link to the base-frame-origin (m) or ZMP

P Total linear momentum (kg.m/s)

P Square symmetric matrix

Q Positive-definite symmetric matrix

R Positive-definite symmetric matrix

R Rotation matrix

t Time (sec)

u Angular acceleration (Input) (rad/s^2)

u Control vector

u_{opt} Optimal control vector

x State vector

x_{ZMP} Distance from ZMP to the base-frame-origin about x-axis (m)

y Output of state space

y_{ZMP} Distance from ZMP to the base-frame-origin about y-axis (m)

z_{ZMP} Distance from ZMP to the base-frame-origin about z-axis (m)

Greek Symbols

J Performance index

θ Angle (rad)

ω Angular acceleration (rad/sec)

τ Torque (N.m)

Abbreviations

CoM Center of mass

CP Capture point

DOF Degree of freedom

FPC Foot positioning compensator

LQR Linear quadratic regulator

ZMP Zero moment point

6. References

1. Thomas B. (2006). *"Embedded Robotics* ". 2nd ed., Springer.
2. Sujan W., Amin B., Nathan S. and Madhavan S. (2012). "*Bipedal Walking Robot - A Developmental Design*", International Symposium on Robotics and Intelligent Sensors (IRIS), Vol. 41, pp. 1016–1021.
3. Miomir V. and Davor J. (1969). *"Contribution to the Synthesis of Biped Gait*", IEEE, Vol. BME-16, No. 1, pp. 1-6.
4. M.V., B.B. and D. S. (1990). *"Biped Locomotion Dynamics, Stability, Control and Application"*. 1st ed., Springer.
5. M.H.P. D. (2009). *"Zero-Moment Point Method for Stable Biped Walking"*. Internship report, Eindhoven, Netherlands, pp. 1–50.
6. Kemalettin E., Akihiro O., Keisuke O., Taro T. and Atsuo K. (2002). "*A Study on the Zero Moment Point Measurement for Biped Walking Robots*". IEEE, pp.431-436.

7. Nima F., Adel A. and Masoud A. (2010), "*ZMP Analysis for Dynamic Walking of a Passivity-based Biped Robot with Flat Feet"*. International Conference on Control, Automation and Systems, PP.1419-1423.
8. Richard C. D. and Robert H. B. (2008) "*Modern Control Systems*". 11th ed. Pearson Prentice Hall, Upper Saddle River, New Jersey.
9. Richard C. D. and Robert H. B. (2010) "*Modern Control Systems*". 12th ed. Pearson Prentice Hall, Upper Saddle River, New Jersey.
10. John D., Bruce F. and Allen T. (1990) "*Feedback Control Theory*". Macmillan Publishing Co.
11. Katsuhiko O. (2010) "*Modern Control Engineering*", 5th ed. Prentice Hall, New Jersey.
12. Ali F. A. and Ahmed A. A. (2019) "*Design of Optimal Stability Linear Inverted Pendulum Model Control for Bipedal Robot*", REVISTA AUS, Vol. 26, pp.529-541.
13. Andre S., and Sabri T. (2006) "*Design of a Biped Robot*". FCRAR, pp.1-6.
14. Young-D. H. (2019) "*Capture Point-Based Controller Using Real-Time Zero Moment Point Manipulation for Stable Bipedal Walking in Human Environment*", Sensors, Vol. 19, pp.1-18.
15. Farid G. and Benjamin C. K. (2010) "*Automatic Control System*", 9th ed., JOHN WILEY & SONS, USA.
16. Chengju L., Tong Z., Ming L., and Qijun C. (2020). "*Active Balance Control of Humanoid Locomotion Based on Foot Position Compensation*". J. Bionic Eng., Vol. 17, pp.134-147.
17. Ali F. A. and Ahmed A. A. (2020) "*Robust Stability Control of Inverted Pendulum Model for Bipedal Walking Robot*", Al-Nahrain Journal for Engineering Sciences NJES, Vol. 23, No.1, pp.81-88.